Vibrational Excitation by Electron Impact near Threshold in H_2, D_2, N_2, and CO†

P. D. Burrow and G. J. Schulz
Mason Laboratory, Yale University, New Haven, Connecticut 06520
(Received 20 May 1969)

The trapped-electron method is applied to the measurement of the slopes of the vibrational cross sections near their respective thresholds. Absolute values are obtained by normalization to positive-ion cross sections. The values obtained in H_2 are 43 for $v=1$, 0.72 for $v=2$, 0.04 for $v=3$, and 0.003 for $v=4$, in units of 10^{-18} cm^2/eV. The values for N_2 are 2.5 for $v=1$ and about 0.02 for $v=2$, whereas, the values for CO are much larger, i.e., 120 for $v=1$ and 2.4 for $v=2$. Various corrections that are necessary for determining absolute cross sections from trapped-electron data are discussed. The validity of the corrections is studied for the case of the 2^3S excitation function in He.

INTRODUCTION

Cross sections for the excitation of vibrational levels of the ground electronic state of diatomic molecules have been previously measured using electrostatic energy analyzers,[1-5] using the trapped-electron method,[6] and using an analysis of swarm experiments.[7-9] A recent review of vibrational and rotational excitation may be found in a paper by Phelps.[10] Electrostatic analyzers have proved to be invaluable in the study of angular dependence, but are relatively insensitive for measurement of small cross sections near threshold. The swarm analysis has produced cross sections for excitation to the first vibrational level which are quite accurate close to threshold, but the method is less accurate at higher energies.

The trapped-electron method,[11] used in the present study, has high sensitivity because it allows complete collection of inelastically scattered electrons and is therefore suitable for the measurement of total inelastic cross sections near threshold. In this paper, we report the absolute cross sections for vibrational excitation of several states of H_2, D_2, N_2, and CO, and we describe changes in the geometry of the tube which give improved operation in the vibrational regime. A discussion is given in Appendixes A and B of two important corrections necessary for the evaluation of absolute cross sections using the trapped-electron method. The validity of the corrections is studied in Appendix C for the case of the 2^3S excitation function in helium.

APPARATUS

The trapped-electron method has been discussed in a number of papers,[11,12] and therefore, only a short description is given here.

Figure 1 shows a schematic diagram of the tube and the variation of potential along the axis. An electron beam, collimated by a magnetic field of about 180 G. is accelerated into the collision chamber with voltage V_A. The collision chamber consists of two end plates and a grid formed of ten thin wires, 0.007 cm diam, strung longitudinally and spaced equally around a circle. A cylindrical outer collector (marked trapped-electron collector in Fig. 1) surrounds the collision chamber. By applying a positive voltage to this collector, with respect to the collision chamber, an electrostatic well, having a depth W (in volts), can be produced along the axis of the tube.

An electron making an inelastic collision just above the threshold for an inelastic process loses most of its energy and is trapped in the well. It spirals back and forth following the magnetic field lines and eventually makes enough elastic collisions to diffuse across the magnetic field to the

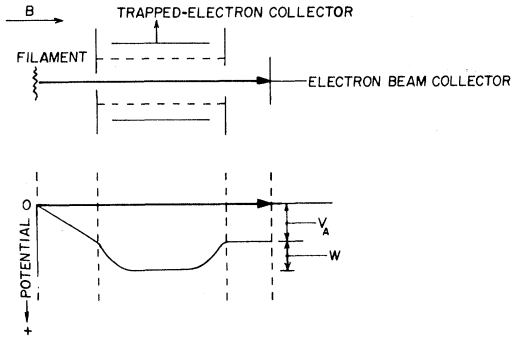

FIG. 1. Schematic diagram of the trapped-electron tube, and the potential distribution along the axis of the tube. The accelerating voltage is given by V_A, and the depth of the well by W.

trapped-electron collector. At an electron energy that exceeds the threshold of an inelastic process by the amount W, the electrons have enough energy remaining to escape through the potential barrier at the end of the collision chamber, and the trapped-electron current vanishes. Therefore, as a function of accelerating voltage, the trapped-electron current is zero below an inelastic threshold, and then grows to a peak which is proportional to the magnitude of the cross section at an electron energy that exceeds the threshold by W.

The usefulness of this technique at low energies has been hampered by the presence of a large strongly varying background current which results from elastically scattered electrons.[6] This arises as follows: For a given well depth, the solid angle into which an elastically scattered electron must be oriented in order to escape becomes smaller as the electron energy decreases. Thus, it becomes increasingly probable that elastically scattered electrons reach the collector as the energy decreases. Because the elastic cross section is generally large, the background current may obscure the smaller current arising from inelastic processes. This effect most likely accounts for the failure to observe vibrational excitation in H_2 of an earlier attempt[11] that used the trapped-electron method.

A portion of the elastically scattered electrons will rescatter with their velocities oriented correctly for escape. However, those electrons which diffuse radially beyond the exit hole of the collision chamber collide with the metal end plates, and a fraction of these is reflected back into the chamber and eventually contributes to the unwanted background current. In the present work, the reflected current has been partially suppressed by enlarging the exit hole of the collision chamber and the two following plates to a diameter of 0.2 cm.

The elastically scattered electrons, which are confined in the collision chamber, have a long effective path length for making inelastic collisions. The correction necessary to take account of this effect is discussed in Appendix A.

The well depth is determined by applying a negative voltage to the trapped-electron collector relative to the collision chamber, thus creating a potential barrier in the path of the electron beam. By measuring the shift in the electron-beam retarding curve for different values of the applied voltage, the size of the barrier is determined. This is the well depth with reversed polarity.

The tube is constructed of Advance metal and molybdenum grid wires with a diameter of 0.007 cm. All metal parts are gold plated to avoid contact potential shifts. The electron gun consists of a thoria-coated iridium filament and three accelerating plates (not shown in Fig. 1). The retarding-potential-difference method[13] is used to produce an electron beam with 0.1 eV width at half-maximum. The tube is mounted in a stainless-steel envelope, and externally mounted Helmholtz coils provide the collimating magnetic field. The tube and vacuum system are baked at 400 °C and reach a background pressure of 1×10^{-9} Torr. Reagent grade gases from high-pressure bottles supplied by the J. T. Baker Chemical Company are used. Continuous flow of the gas is maintained in order to minimize the buildup of impurity gases in the collision chamber. The pressure in the collision chamber is typically 1×10^{-3} Torr. In this pressure region, the trapped-electron current shows a linear dependence on pressure.

RESULTS

Figure 2 shows the trapped-electron current as a function of electron energy in H_2, measured with a well depth of 0.07 V. The elastic background current is present at energies below 0.3 eV. The two peaks in Fig. 2 are associated with the excitation to the first and second vibrational levels near their thresholds at 0.52 and 1.01 eV, respectively.[14] The energy scale is determined by the appearance potential of positive ions and is considered reliable within 0.15 eV. The height

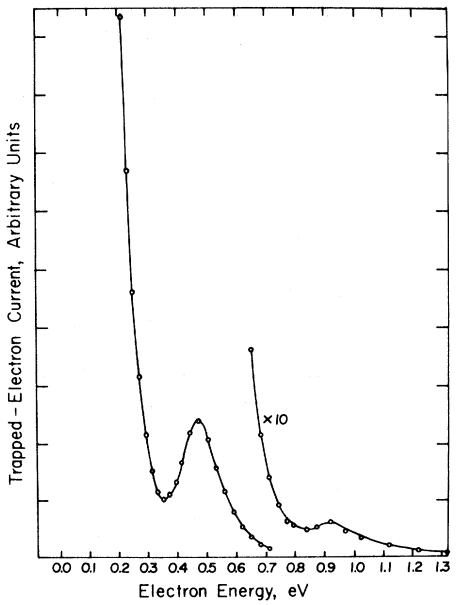

FIG. 2. Energy dependence of the trapped-electron current in H_2 measured with a well depth of 0.07 V. The sharply rising current below 0.3 eV is due to the elastically scattered background current. The two peaks at higher energies represent excitation to the first and second vibrational levels.

of the peaks shown in Fig. 2 is proportional to the excitation cross section at an energy above threshold equal to the well depth. By taking several sweeps with different well depths, the cross section can be observed as a function of energy.

As the well depth increases, the elastic peak grows rapidly, eventually overwhelming the peaks due to excitation to the lower vibrational levels. For this reason, the largest well depth used here is about 0.12 V. The third and fourth vibrational levels in H_2, discussed below, are the only exceptions. Because they are far removed in energy from the elastic peak and are well separated from each other, they can be traced to 0.35 eV above threshold.

Absolute magnitudes are assigned to the cross sections by comparing the trapped-electron signal with the positive-ion signal at 40 eV and normalizing to the ionization cross sections measured by Rapp and Englander-Golden.[15] The values thus obtained are corrected for the finite energy spread of the electron beam, as described in Appendix B, and for the effective path length resulting from confined elastically scattered electrons, as described in Appendix A.

Data similar to that shown in Fig. 2 are also taken for excitation to the first and second vibrational levels in D_2, N_2, and CO. These measurements are made with well depths below 0.12 V, and within experimental error are consistent with a cross section having a linear energy dependence over this narrow range. The slopes of these cross sections just above threshold are tabulated in Table I. The error in these values (±50%) results largely from the uncertainty in subtracting the contribution of the elastic background current.

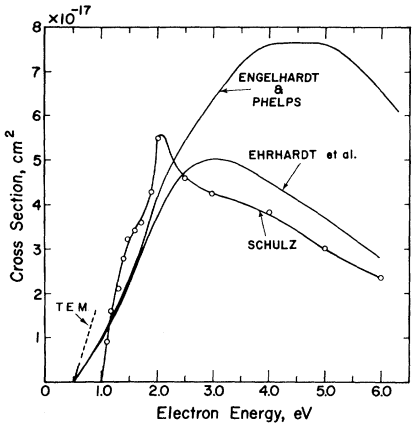

FIG. 3. Comparison of the data for the excitation of the first vibrational level in H_2 as a function of energy. The slope of the cross section found by the trapped-electron method (TEM) is shown by the dashed line. The cross section is measured only for the first 0.1 eV above threshold.

DISCUSSION

A. H_2

Figure 3 shows the data for excitation to the first vibrational level in H_2. The dashed line indicates the slope of the cross section measured within 0.1 eV of threshold using the trapped-electron method. Also shown are the electrostatic analyzer data of Schulz,[1,16] Ehrhardt *et al.*,[5] and the cross section deduced from an analysis of swarm data by Engelhardt and Phelps.[7] The present data indicate a large cross section near threshold. This confirms the analyzer data of Menendez and Holt[2] and Ehrhardt *et al.*,[5] who found an excitation function which increases monotonically from threshold up to its maximum. Recent data by Boness and Schulz[17] obtained in a double electrostatic analyzer are also in agreement with this result. The delayed onset previously observed by Schulz[1] using a double electrostatic analyzer was apparently due to a lower signal-to-noise ratio near threshold.

Vibrational excitation to $v = 2$ is shown in Fig.4, together with the analyzer data of Schulz,[1] and Ehrhardt *et al.*[5] By broadening the electron energy distribution to about 0.2 eV width at half-maximum and using higher beam current, it is possible to measure excitation to the third and fourth vibrational levels near threshold. Figure 5 shows the result for $v = 3$, in comparison with the analyzer data of Ehrhardt *et al.*[5] The trapped-electron data are shown with open circles. The dashed line is a reasonable interpolation between the two sets of data.

There are no other data with which to compare

TABLE I. Slope of the cross section for vibrational excitation near threshold, in cm^2/eV.

	H_2	D_2	N_2	CO
$v=1$	4.3×10^{-17}	2.0×10^{-17}	2.5×10^{-18}	1.2×10^{-16}
$v=2$	7.2×10^{-19}	3.5×10^{-19}	$\sim2\times10^{-20}$	2.4×10^{-18}
$v=3$	4×10^{-20}			
$v=4$	3×10^{-21}			

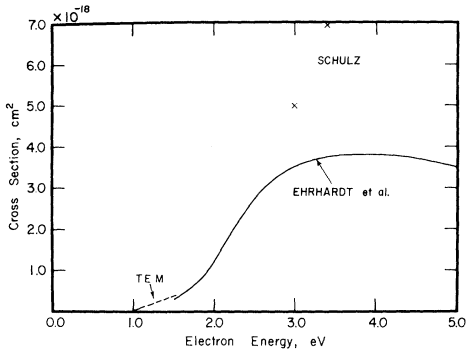

FIG. 4. Comparison of the data for the excitation of the second vibrational level in H_2 as a function of energy. The slope of the cross section found by the trapped-electron method (TEM) is shown by the dashed line. The cross section is measured only for the first 0.1 eV above threshold.

our results for excitation to $v = 4$. The energy dependence of the cross section over the 0.35-eV range above threshold is similar to that for $v = 3$. The slope at threshold is given in Table I.

Excitation to the vibrational levels is assumed to take place through the formation of a temporary negative-ion state,[1] H_2^-, with a lifetime estimated to be 1×10^{-15} sec.[18] The cross section for excitation to this state has a maximum in the vicinity of 2 eV. However, the large cross section for excitation to $v = 1$ at threshold indicates that excitation to the temporary ion state[19] is broad enough to overlap the $v = 1$ level at 0.5 eV.

The cross section at threshold for excitation to $v = 1$, measured here, lies above that found by Engelhardt and Phelps,[7] and Ehrhardt *et al.*[5] Although the error limits overlap slightly, it is not clear at present whether the difference is significant. Agreement with the data of Ehrhardt *et al.*[5] for excitation to $v = 2$ and $v = 3$ is good.

B. D_2

The cross sections to the first and second vibrational levels of D_2 near threshold are found to be 47% of the corresponding cross sections in H_2. This is in good agreement with the figure of 54% obtained by Engelhardt and Phelps[7] for excitation to $v = 1$ in D_2 and H_2. As in the case of H_2, however, the absolute magnitude of the cross section measured in D_2 is larger than that found by using the swarm analysis.

Vibrational excitation in D_2, as in H_2, proceeds through the formation of a temporary negative ion. The cross section for excitation to the temporary state is expected to be nearly the same in both gases. The smaller cross section for vibrational excitation in D_2 near threshold most likely results from the larger separation of its threshold at 0.36 eV, from the maximum for excitation of the temporary negative ion at 2 eV. No pronounced isotope effect such as that occurring in the dissociative attachment[18] of electrons in H_2 and D_2 is expected. Almost all of the excitation to the temporary negative-ion state results in population of the ground and lower vibrational levels. Dissociative attachment, therefore, is unimportant as a competing process.

C. N_2

Data for excitation to $v = 1$ in N_2 are shown in Fig. 6, with the cross sections deduced from swarm data by Engelhardt, Phelps, and Risk[8] and the low-energy portion of the analyzer data by Schulz.[1] The sharply increasing cross section observed above 1.5 eV represents the contribution of the temporary negative-ion state N_2^-, which lies near 2.3 eV. This state has a relatively long lifetime and well-developed vibrational structure. The excitation to $v = 1$ and higher vibrational levels of N_2, which proceeds through this state, has been studied in detail by Schulz,[1,3] and Ehrhardt and Willman.[4]

The small cross section at threshold may result from direct excitation and from any residual tailing of the temporary negative-ion state extending to 0.29 eV. According to Phelps,[10] the low-energy portion of Chen's theoretical cross section[20] is identical to that of Engelhardt, Phelps, and Risk[8] below 1.2 eV.

The trapped-electron data show no evidence for the curvature in the cross section just above threshold. The scatter in the data due to sub-

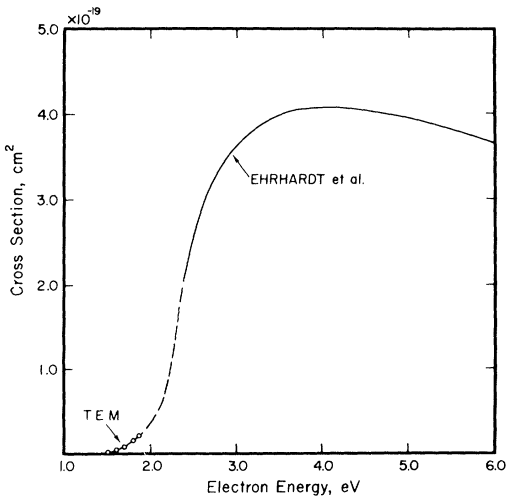

FIG. 5. Comparison of the data for the excitation of the third vibrational level in H_2 as a function of energy. The trapped-electron data are shown by the open circles. The dashed line is a reasonable interpolation between the present data and those of Ehrhardt *et al.*

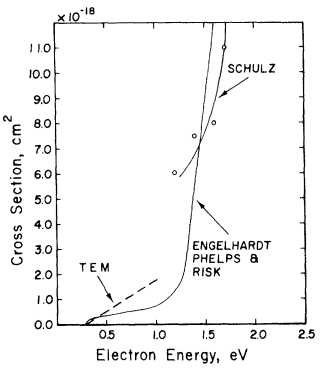

FIG. 6. Comparison of the data for the excitation of the first vibrational level in N_2 as a function of energy. The slope of the cross section found by the trapped-electron method is shown as a dashed line. The cross section is measured only for the first 0.1 eV above threshold.

traction of the elastic background current may make this feature difficult to observe.

Excitation to the $v = 2$ level in N_2 is observable but difficult to measure because of its small size and because of the small separation in energy from the $v = 1$ level. The cross section at threshold is estimated to be 1% of that for the $v = 1$ level.

D. CO

Data for the excitation to $v = 1$ in CO are shown in Fig. 7, in comparison with the data of Schulz,[1] Ehrhardt *et al.*[5] and Hake and Phelps.[9] As in the case of N_2, no curvature at threshold could be observed within the error caused by the large background current.

Carbon monoxide, being isoelectronic with N_2, also possesses a compound state which dominates vibrational excitation at energies between 1.2 and 3 eV.[1] The structure in the vibrational excitation at these energies is less pronounced than in N_2, indicating a shorter lifetime of the temporary negative ion, and thus a broader energy range over which excitation takes place. The excitation at threshold may therefore contain a larger contribution from the compound state than in N_2. The dominant means of excitation at threshold, however, should result from the electric dipole moment possessed by CO. This is substantiated by the agreement of the cross section below 1 eV for excitation to $v = 1$, deduced by Hake and Phelps,[9] and the simple Born-approximation calculation also discussed in their paper. The present data show that the cross section at threshold is 50 times larger than that in N_2.

The cross section for excitation to $v = 2$, which was neglected in the swarm analysis, is expected to be smaller by 3.5×10^{-3} than that for excitation to $v = 1$, if the Born approximation is valid.[9] The trapped-electron data give a ratio of 1.9×10^{-2} for the slopes at threshold. This suggests that excitation to the second vibrational level, which is closer to the temporary negative-ion state, may be larger than predicted by direct excitation alone.

CONCLUSION

In this work, the trapped-electron technique is applied to the study of vibrational excitation near threshold. The results indicate for H_2 and D_2 that the vibrational cross section at threshold may be considerably enhanced by the presence of a broad temporary negative-ion state, centered 2 eV higher. In the case of N_2, the temporary negative-ion state is considerably narrower, and its influence at threshold is proportionately smaller. Although a similar temporary negative-ion state exists in CO, excitation at threshold is dominated by the molecular electric dipole moment.

ACKNOWLEDGMENTS

The authors are indebted to M. J. W. Boness, J. L. Mauer IV, D. Spence, and A. Stamatovic for many stimulating discussions, and to A. V. Phelps for valuable comments.

APPENDIX A: CORRECTIONS FOR EFFECTIVE PATH LENGTH

In this section, we discuss the effect of the elastically scattered electrons on the measurement of

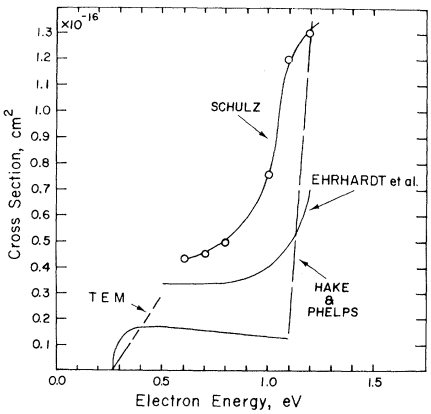

FIG. 7. Comparison of the data for the excitation of the first vibrational level in CO as a function of energy. The slope of the cross section found by the trapped-electron method is shown by the dashed line. The cross section is measured only for the first 0.08 eV above threshold. The portion of the data of Hake and Phelps shown with long dashes is only approximate. Vibrational excitation at energies above about 1 eV could not be determined because of the absence of appropriate experimental electron transport data.

the vibrational cross section. At low electron energy, a fraction of the main electron beam is scattered elastically into a solid angle such that the axial component of electron velocity is insufficient for escape through the potential barrier at the ends of the collision chamber. These electrons spiral along the magnetic field lines and repeatedly traverse the collision chamber. Successive elastic collisions orient most of these electrons correctly for escape, but a few electrons are always trapped and eventually migrate to the trapped-electron collector. At any time in this sequence, an electron may make an inelastic collision and contribute to the trapped-electron signal. The measured inelastic cross section is therefore larger than the true value. Because the fraction of the main beam which scatters elastically is small, one might expect the correction to be unimportant. Although the scattered electrons are indeed few in number, they have very long path lengths compared to the main beam. At the energies and well depths used in this work, the correction cannot be neglected.

The effective beam current may be calculated in the following way: Let I_0 equal the main electron-beam current, N equal the density of molecules in the collision chamber, Q_e equal the total elastic scattering cross section, l equal the path length of the collision chamber, λ equal the mean free path for elastic scattering, W equal the well depth in volts, and E equal the electron energy in the collision chamber in eV.

In order for electrons in the main beam to scatter elastically and be temporarily trapped, they must scatter at an angle greater than a certain critical angle θ_c, measured with respect to the tube axis. It is easily shown that

$$\cos\theta_c = (W/E)^{1/2} \quad .$$

Furthermore, it follows for the case of isotropic elastic scattering, that the fraction of the elastically scattered electrons which is temporarily trapped after the first collision is given by $(W/E)^{1/2}$.

Therefore, the electron current, which is temporarily trapped after the first elastic collision, provided that $NQ_0 l \ll 1$, is given by

$$I_0 NQ_e l(W/E)^{1/2}.$$

We also assume that the elastic cross section is larger than the inelastic. On the average, these trapped electrons move a length equal to the elastic mean free path λ before rescattering. Relative to the main beam current, the scattered beam current must be weighted by a factor of $\lambda/l = (NQ_e l)^{-1}$.

We have at this point an effective beam current given by

$$I_0 + I_0 NQ_e l(W/E)^{1/2}(NQ_e l)^{-1} .$$

After several successive elastic collisions, the effective beam current is given by

$$I_0[1 + (W/E)^{1/2} + (W/E) + (W/E)^{3/2} + \cdots] .$$

Because W is always less than E, the higher terms become smaller. Although only a finite number of collisions take place, we may sum the series over an infinite number of terms to good approximation. The effective beam current then becomes

$$I_0[1 - (W/E)^{1/2}]^{-1} .$$

This yields immediately the relation between the true cross section and the measured cross section

$$Q_{\text{true}} = [1 - (W/E)^{1/2}]Q_{\text{measured}}.$$

As an example, for the case where $W = 0.1$ V and $E = 0.5$ eV, the measured cross section must be multiplied by the factor of 0.55.

Unfortunately, this simple analysis is only correct for elastic scattering which is isotropic. If the first elastic scattering event takes place more strongly in the forward direction, this will lower the amount of the current which is temporarily trapped. In this case, the correction used above gives a cross section which is smaller than the true value. Because the angular dependence of the elastic scattering in molecules is not generally known at low energies, the data given in the body of this paper are corrected using the assumption of isotropic scattering.

APPENDIX B: CORRECTIONS FOR FINITE ENERGY DISTRIBUTION

Because the well depths used in this work are comparable to the energy spread of the electron beam, considerable broadening of the trapped-electron peaks occurs. Unless corrected, this would lead to an underestimate of the inelastic cross section. The following calculations[21] were made in order to indicate the range of well depths (relative to the energy spread) for which sizable correction must be employed.

The trapped-electron current as a function of energy is derived for the special case of an inelastic process with a cross section increasing in a linear manner above threshold and an electron beam having a Gaussian distribution of energies with a full width at half-maximum of ΔE eV.

For the particular case in which the spread of electron energy is equal to half the well depth, that is, $\Delta E = \frac{1}{2}W$, the trapped-electron peak shape is illustrated in Fig. 8. Also shown is the theoretical curve for infinitely good energy resolution $\Delta E = 0$. The decrease in energy resolution produces a large change in the maximum value of the trapped-electron current. In addition, the position of the peak is shifted to a lower energy.

We can take the ratio of the trapped-electron peak height for a finite electron-energy distribution to the peak height for an infinitely narrow distribution and plot it as a function of the ratio of the well depth to the half-width of the electron energy distribution. Such a plot gives an indication of the range of well depths over which sizable error occurs. This is shown in Fig. 9. Note that this curve is applicable only when the cross section increases linearly and when the electron-energy distribution is Gaussian. Only for $W > 1.6\,\Delta E$ does the error drop below 50%. If the electron distribution is known, the correction factor for a given well depth may be found from curves similar to that in Fig. 8 which are easily calculated.

A second method for correction derives from the observation that the area under the broadened trapped-electron curve is the same as that under the curve for monoenergetic electrons. Knowing the well depth, the corrected peak height can be found graphically. Because the experimentally measured electron distribution is not a convenient analytic function, this method is more easily carried out, and is used for evaluating the vibrational cross sections given in the text.

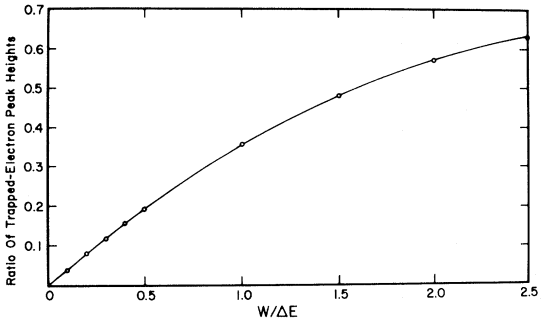

FIG. 8. Computed trapped-electron peak shape as a function of electron energy. These curves are derived for the special case of an inelastic process having a cross section which increases in a linear manner above threshold. The triangular peak is the result for an infinitely narrow electron-energy distribution. The curve shown with open circles is the result for a Gaussian energy distribution with a half-width of $\frac{1}{2}W$.

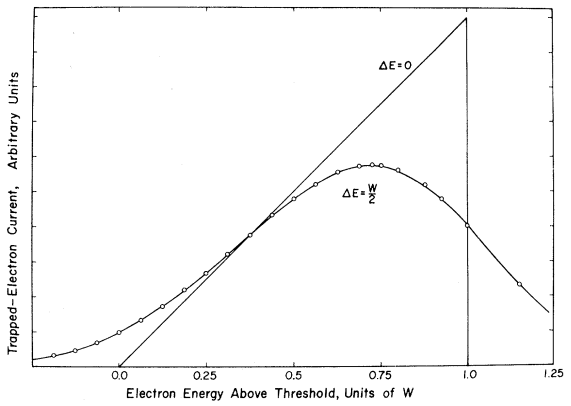

FIG. 9. Ratio of the trapped-electron peak height for a finite electron-energy distribution to the peak height for an infinitely narrow distribution, as a function of the ratio of the well depth to the half-width of the energy distribution. For a given value of the well depth and half-width, this curve indicates the extent to which the cross section is underestimated. These curves are computed for the special case of a linear cross section above threshold and a Gaussian electron-energy distribution.

APPENDIX C: EXPERIMENTAL TESTS OF THE CORRECTIONS

To demonstrate the validity of the corrections discussed in Appendixes A and B, we apply them to the measurement of excitation to the 2^3S state in helium by the trapped-electron method. To isolate the effect of each of the corrections, we have chosen two examples, in which one correction is necessary and the other may be neglected.

First we consider the correction discussed in Appendix A for the increased effective path length due to elastically scattered electrons. In a study of excitation using large well depths, Schulz[12] found that the apparent cross section at an impact energy of 20.4 eV was larger than that measured by other means,[22] by an amount which depended on the well depth. Using a well depth of 0.69 V, the cross section was 14% larger; using 1.6 V, the cross section was 50% larger. Applying the correction derived in Appendix A, we must multiply the apparent cross sections by factors of 0.827 and 0.721, respectively. This yields cross sections which are 94 and 108%, respectively, of the true value. Because both well depths are large compared with the half-width of the electron-energy distribution, the relative correction for broadening discussed in Appendix B is negligible.

The correction for the finite electron-energy distribution discussed in Appendix B is tested on a measurement of the cross section for excitation

to the 2^3S state near its threshold at 19.8 eV. The peaks of the trapped-electron current have been measured at several well depths from 0.040 to 0.1 V with an electron-energy spread of 0.2 eV. In this case, $W/E \sim 0.005$ and the corrections discussed in Appendix A are too small to be significant. However, $W/\Delta E < 0.5$ and, from Fig. 9, it is obvious that a correction for the finite electron-energy distribution is required. Using the area method described in Appendix B, the corrected trapped-electron current at its peak is calculated. The absolute cross section is found by referring the trapped-electron current to the positive-ion current produced at 40 eV and using the ionization cross section of Rapp and Englander-Golden.[15] The resulting data yield a slope at threshold of $1.6\times10^{-17}\pm30\%$ cm^2/eV.

The total metastable cross section has been measured by Schulz and Fox[23] to be 4×10^{-18} cm^2 $\pm30\%$, at its peak at 20.4 eV. Using their excitation function, this gives a threshold slope of 1.1×10^{-17} cm^2/eV $\pm30\%$. The relative cross section has been measured also by Pichanick and Simpson[24] with better electron-energy resolution. By assigning a value of 4×10^{-18} cm^2 to the peak of the relative cross section of Pichanick and Simpson, we obtain from their data a slope at threshold of 1.5×10^{-17} cm^2/eV $\pm30\%$. The increased slope is most likely due to the improved electron-energy distribution in the experiment of Pichanick and Simpson. The value for the slope of the 2^3S excitation function near threshold, obtained in the present experiment using the trapped-electron method with the appropriate correction, is thus in good agreement with the value obtained from Pichanick and Simpson.

In conclusion, it is felt that the correction procedures outlined in Appendixes A and B are justified, and yield fairly reliable ($\pm10\%$) values for cross sections near threshold.

---

†Work supported by the Advanced Research Projects Agency through the Air Force Office of Scientific Research.

[1]G. J. Schulz, Phys. Rev. 135, A988 (1964).

[2]M. G. Menendez and H. K. Holt, J. Chem. Phys. 45, 2743 (1966).

[3]G. J. Schulz, Phys. Rev. 125, 229 (1962).

[4]H. Ehrhardt and K. Willman, Z. Physik 204, 462 (1967).

[5]H. Ehrhardt, L. Langhans, F. Linder, and H. S. Taylor, Phys. Rev. 173, 222 (1968).

[6]G. J. Schulz and J. T. Dowell, Phys. Rev. 128, 174 (1962).

[7]A. G. Engelhardt and A. V. Phelps, Phys. Rev. 131, 2115 (1963).

[8]A. G. Engelhardt, A. V. Phelps, and C. G. Risk, Phys. Rev. 135, A1566 (1964).

[9]R. D. Hake, Jr., and A. V. Phelps, Phys. Rev. 158, 70 (1967).

[10]A. V. Phelps, Rev. Mod. Phys. 40, 399 (1968).

[11]G. J. Schulz, Phys. Rev. 112, 150 (1958).

[12]G. J. Schulz, Phys. Rev. 116, 1141 (1959).

[13]R. E. Fox, W. M. Hickam, D. J. Grove, and T. Kjeldaas, Rev. Sci. Instr. 26, 1101 (1955).

[14]G. Herzberg, Spectra of Diatomic Molecules (D. Van Nostrand Co., Inc., Princeton, New Jersey, 1950).

[15]D. Rapp and P. Englander-Golden, J. Chem. Phys. 43, 1464 (1965). Normalization to the positive-ion cross section is performed to the values of Rapp and Englander-Golden. However, it seems that none of the determinations of the absolute cross sections have taken into account the error produced by the emission of secondary electrons resulting from potential ejection by the incident ions. Even if the values in the literature had been corrected for this effect, it is by no means certain that the present experiment is free from this effect. Thus, any normalization in this manner is subject to an error which may be as large as 20% for ions with a high ionization potential (e.g., helium). It appears to us that negative-ion cross sections are not afflicted by this consideration and thus may be more reliable as a standard.

[16]J. N. Bardsley, A. Herzenberg, and F. Mandl [Proc. Phys. Soc. (London) 89, 321 (1966)] state that Schulz's data should be multiplied by 1.4 to correct for the non-isotropic nature of the inelastic scattering. However, this was based on the assumption that the inelastic scattering cross section had been measured absolutely when, in fact, it was measured with respect to the elastic cross section. Because the angular distribution of elastic scattering is not known, the correction factor is not well established, and the data quoted here are unaltered.

[17]M. J. W. Boness and G. J. Schulz (unpublished).

[18]G. J. Schulz and R. K. Asundi, Phys. Rev. 158, 25 (1967).

[19]Although direct-excitation calculations using the Born approximation and including polarization also give large cross sections near threshold [see E. L. Breig and C. C. Lin, J. Chem. Phys. 43, 3839 (1965)], the compound-state model must be preferred at the present time. The latter predicts correctly the ratio of the higher vibrational excitations and the magnitude of the dissociative-attachment cross section at 3.6 eV, which proceeds via the same compound state [see J. N. Bardsley, A. Herzenberg, and F. Mandl, Proc. Phys. Soc. (London) 89, 321 (1966)].

[20]J. C. Y. Chen, J. Chem. Phys. 40, 3507 (1964).

[21]The authors are very much indebted to John L. Mauer IV for writing the computer program and doing much of the analysis in Appendix B.

[22]H. Maier-Leibnitz, Z. Physik 95, 499 (1936).

[23]G. J. Schulz and R. E. Fox, Phys. Rev. 106, 1179 (1957).

[24]F. M. J. Pichanick and J. Arol Simpson, Phys. Rev. 168, 64 (1968).

PHYSICAL REVIEW VOLUME 187, NUMBER 1 5 NOVEMBER 1969

Discrete Deposition of Energy by Electrons in Gases*

Lennart R. Peterson
University of Florida, Gainesville, Florida 32601
(Received 9 June 1969)

Much previous work on the energy deposition of electrons in gases has centered on the continuous-slowing-down approximation, the key element being the loss function $-(1/n)dE/dx$. Calculations generally reduce to energy integrals involving cross sections and this loss function. The limits of the continuous approximation are now examined by comparing it over various energy intervals with a method which takes into account the discrete nature of the energy lost in each collision. The calculation at each stage considers how an electron at a particular energy will redistribute itself on average at all lower energies, with the distribution depending on cross sections and transition energies. Results of the present work for He and N_2, and comparisons to the continuous approximation, are given.

I. INTRODUCTION

An important aspect of upper atmospheric research involves the question of how an energetic electron incident on a gas populates the various atomic and molecular states it can excite. For example, recent studies of this nature, applied to the calculation of spectral intensities of auroral and dayglow lines, have been carried out by several authors.[1–4] For reasons of its great convenience, the continuous-slowing-down approximation (CSDA) is generally used in these applications whereas the real situation is more in the nature of a random-walk problem. Here the electrons degrade their energy by a series of quantum jumps rather than by the CSDA assumption of continuous energy loss.

The question of how well the CSDA does is, of course, not a new one. Wilson[5] in the precomputer era of physics studied electron and photon initiated showers in lead by Monte Carlo probability wheel methods. Fano[6] and Spencer and Fano[7] in an analysis of range and energy loss of ionizing radiations in matter were concerned with the effects of occasional very large losses due to bremsstrahlung. They discussed an integral equation describing the discrete loss and then combined approximate solutions of it with CSDA to obtain a scheme involving both descriptions.

What is needed for present purposes is a careful examination of CSDA at all energies of interest to atmospheric physics. It is clear that for a sufficiently low-energy electron incident on a gas, the CSDA will predict too small an energy given up to the various states on average. This point may be illustrated convincingly by considering the energy loss of a 25-eV electron in helium. Helium is a rather special case among atmospheric gases in that all the cross sections describing single-electron excitations or ionizations have thresholds bunched together between 19.8 and 24.6 eV. Thus a 25-eV electron will on average lose 22 or 23 eV on its first (and only) collision. On the other hand, the CSDA, which involves an integration over energy from 25 eV down to the lowest threshold at 19.8, predicts a loss of only about 5 eV. The arguments just presented for He do not lead to such obvious conclusions when applied to gases having thresholds widely distributed in energy nor when applied to high energies. Further complications are present when the incident particles have a spectrum of energies.

The present study investigates under what conditions the CSDA is valid with respect to applied problems. The model gases are He and N_2 using the complete sets of semiempirical cross sections given by Jusick *et al.*[8] for He and tabulated by Peterson *et al.*[9] for N_2. Only cross sections for electronic transitions have been included, but, as will be indicated in the results, the inclusion of other cross sections tends to make the continuous approximation more, rather than less, reliable. Hence the results of this work indicate an upper limit to the discrepancies.